FINAL REPORT

on

CRYSTALLIZATION, FLOW AND THERMAL HISTORIES OF LUNAR AND TERRESTRIAL COMPOSITIONS

Submitted to

NATIONAL AERONAUTICS AND SPACE ADMINISTRATION

on

RESEARCH GRANT NGR 22-009-646

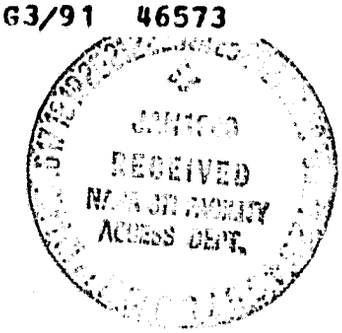

INTRODUCTION

Work on the grant was initiated in June, 1971 and was carried out through August 1979. The work resulted in some 50 technical publications, a list of which is appended to the present report.

Our activity during the period of the grant was concerned with 22 principal objectives:

I. A Kinetic Treatment of Glass Formation

II. Effects of Nucleating Heterogeneities on Glass Formation

III. Glass Formation under Continuous Cooling Conditions

IV. Crystallization Statistics

V. Kinetics of Crystal Nucleation

VI. Diffusion Controlled Crystal Growth

VII. Crystallization of Lunar Compositions

VIII. Crystallization Between Solidus and Liquidus

IX. Crystallization on Reheating a Glass

X. Temperature Distributions during Crystallization

XI. Crystallization of Anorthite and Anorthite-Albite Compositions

XII. Effect of Iron Oxidation State on Viscosity

XIII. Diffusive Creep and Viscous Flow

XIV. High Temperature Flow Behavior of Glass-Forming Liquids, a Free Volume Interpretation

XV. Viscous Flow Behavior of Lunar Compositions

XVI. Thermal History of Orange Soil Material

XVII. Breccia Formation by Viscous Sintering

XVIII. Viscous Sintering

XIX. Thermal Histories of Breccias

XX. Solute Partitioning and Thermal History of Lunar Rocks

XXI. Heat Flow in Impact Melts

XXII. Thermal Histories of Olivines

The support by the grant made it possible to examine each of these areas in detail. It also provided the basis for fruitful collaboration between workers in our group of materials scientists and geologists in other institutions. As will be seen from the report below, a significant portion of the work was carried out in such a collaboration spirit, with Dr. Simonds of the Lunar and Planetary Institute, Dr. Lofgren of the Johnson Space Center, Professor Hays of Harvard, Professor Kirkpatrick of the University of Illinois, and Professor Taylor of the University of Tennessee. Interaction with these individuals, as well as others in the Lunar and Planetary Program, has been perhaps the most rewarding aspect of our participation in the program.

For these reasons, we wish to express again our appreciation to NASA for their support.

I. A KINETIC TREATMENT OF GLASS FORMATION

The results of many investigations have indicated that glass-forming liquids have been found in every category of material based on bond type, including covalent, ionic, metallic, van der Waals and hydrogen. In this light, and in light of the occurrence of either glassy or crystalline forms of a given specimen depending upon the conditions of its formation, it seems appropriate to inquire not whether a material will form a glass when cooled in bulk form from the liquid state, but rather how fast must it be cooled in order that detectable crystallization be avoided.

In attempting to answer this question and better understand the formation of glasses and various phase assemblages in the lunar environment, an analysis has been carried out of the kinetic conditions for glass formation. This analysis as carried out to date has been concerned with two questions: (1) how small a volume fraction of crystals embedded in a glassy matrix can be detected and identified; and (2) how can the volume fraction of crystals be related to the kinetic constants describing the nucleation and growth process, and how can these kinetic constants in turn be related to readily-measurable parameters?

In answering the first of these questions, we have been concerned with crystals which are distributed randomly through the bulk of the liquid, and have identified a volume fraction of 10^{-6} as a just-detectable concentration of crystals. The estimated cooling rates will not depend strongly on this assumed detectability limit, and our concern

with crystals distributed throughout the glass provides an estimate of the necessary rather than a sufficient cooling rate for glass formation.

In answering the second question, we have adopted the formal theory of transformation kinetics developed originally by Johnson and Mehl and Avrami. Taking the rate of crystal growth and the nucleation frequency as constant with time, the volume fraction, X, crystallized in a time, t, may for small X be expressed:

$$X \approx \frac{\pi}{3} I_v u^3 t^4 \qquad (1)$$

Here I_v is the nucleation frequency per unit volume and u is the rate of advance of the crystal-liquid interfaces per unit area of the interfaces.

In identifying I_v as the steady-state rate of homogeneous nucleation, we have neglected heterogeneous nucleation events--such as at external surfaces--and have been concerned with minimum cooling rates for glass formation. Clearly, a glass cannot be formed if observable amounts of crystals form in the interiors of samples. We shall also neglect the effect of transients during which the steady-state concentrations of subcritical emryos are built up by a series of bimolecular reactions. This neglect is generally justified whenever the time required to establish the steady-state nucleation rate is small relative to the total transformation time and to the time scale of the observations. This is expected to maintain in nearly all cases of cooling liquids to form glasses.

The cooling rate required to avoid a given volume fraction crystallized may be estimated from Equation (1) by the construction of so-called T-T-T (time-temperature-transformation) curves, examples of which are shown in Ref. 1. In constructing these curves, a particular fraction crystallized is selected, the time required for that volume fraction to

form at a given temperature is calculated and the calculation is repeated for other temperatures (and possibly other fractions crystallized).

The nose in a T-T-T curve, corresponding to the least time for the given volume fraction to crystallize, results from a competition between the driving force for crystallization, which increases with decreasing temperature, and the atomic mobility, which decreases with decreasing temperature. Using the familiar assumption of additivity, in avoiding a given fraction crystallized, one must cool at a rate such that:

$$\sum_i \frac{dt_i}{t_i} < 1 \qquad (2)$$

Here dt_i is the time for which the sample is in the temperature range between T_i and $(T \pm dT)_i$, and t_i is the time at that temperature required for the given fraction crystallized.

The transformation times, t_i, are relatively long in the vicinity of the melting point as well as at low temperatures, and the principal contributions to the sum in Eqn. (2) come from temperatures in the vicinity of the nose. For purposes of the present analysis, then, we have approximated the cooling rate required to avoid a given fraction crystallized by the relation:

$$\left(\frac{dT}{dt}\right)_c \approx \frac{\Delta T_N}{\tau_N} \qquad (3)$$

where $\Delta T_N = T_E - T_N$; T_N = temperature at the nose of the T-T-T curve; and τ_N = time at the nose of the T-T-T curve.

From the form of Eqn. (1), as well as from the curves shown in Ref 1, which were calculated therefrom, it is apparent that the cooling

rate required for glass formation is rather insensitive to the assumed volume fraction crystallized, since the time at any temperature on the T-T-T curve varies only as the one-fourth power of X.

An alternative estimate of the glass-forming characteristics of materials may be obtained by considering the thickness of sample which can be obtained as an amorphous solid. Again using the criterion of a volume fraction crystallized less than 10^{-6}, and neglecting problems associated with heat transfer at the external surfaces of the sample, the thickness, y_c, of sample which can be formed without detectable crystallization should be of the order:

$$y_c \approx (D_{TH}\ \tau_N)^{1/2} \qquad (4)$$

where D_{TH} is the thermal diffusivity of the sample. For most silicate glasses at temperatures below the range of high radiant conductivity, or for highly absorbing glasses such as those with a high iron content, D_{TH} is in the range 3 to 7 x 10^{-3} cm^2 sec^{-1}.

In estimating the critical conditions for forming a glass of a given material, one can in principle employ measured values of the kinetic factors in calculating the T-T-T curves. In practice, however, information on the temperature dependence of the nucleation frequency is almost never available; and in only a portion of the cases of interest are adequate data available on the variation of the growth rate with temperature. In nearly all cases, therefore, it is necessary to estimate the nucleation frequency from the standard model for homogeneous nucleation; and in some instances it is convenient to estimate the growth rate from standard theoretical models as well.

For describing nucleation in glass-forming systems, the nucleation frequency may be expressed:

$$I_v \approx N_v^{\circ} \nu \exp - \frac{1.024}{T_r^{3} \Delta T_r^{2}} \qquad (5)$$

Here N_v° is the number of single molecules per unit volume; ν is the frequency coefficient for transport at the nucleus-liquid interface; $T_r = T/T_E$; T_E is the melting point or liquidus temperature; ΔT is the undercooling ($\Delta T = T_E - T$); and $\Delta T_r = \Delta T/T_E$.

In obtaining this relation, it was assumed that the free energy of forming the critical nucleus is 50 kT at $\Delta T_r = 0.2$ (in consonance with experimental results on a wide variety of materials) and that the motivating potential for crystallization, ΔG, can be related to the heat of fusion, ΔH_f, by the relation $\Delta G = \Delta H_f \, \Delta T_r \, T_r$.

The rate of advance of a crystal-liquid interface, per unit area of the interface, may be expressed:

$$u = f \nu_g a_o \left[1 - \exp \left(- \frac{\Delta H_{fM} \, T_r}{RT}\right)\right] \qquad (6)$$

Here f is the fraction of sites on the interface where atoms may preferentially be added and removed; ν_g is the kinetic coefficient for transport at the crystal-liquid interface; ΔH_{fM} is the heat of fusion per gram atom and a_o is a molecular diameter.

For materials with small entropies of fusion ($\Delta H_{fM}/T_E < 2R$), the interface is expected to be rough on an atomic scale and f should be of the order unity and should not vary significantly with undercooling. For materials with large entropies of fusion ($H_{fM}/T_E > 4R$), the interface is expected to be smooth on an atomic scale and growth should take

place at steps provided by screw dislocations or two-dimensional nuclei formed on the interface. In the former case, which may be anticipated for imperfect crystals, f may be expressed:

$$f \approx 0.2\ \Delta T_r \tag{7}$$

In using Eqn. (5) to evaluate the nucleation frequency, it is customary to take ν as inversely related to the viscosity, η. For purposes of the present calculations, we have taken this proportionality coefficient as the Stokes-Einstein coefficient.

$$\nu = b/\eta \tag{8}$$

where

$$b = kT/3\ a_o^3$$

In cases where growth rate data are not available for a given material, ν_g is generally taken equal to ν.

Combining Eqns. (1), (5), (6) and (8), the time corresponding to a given volume fraction crystallized can be estimated for any desired temperature and the appropriate T-T-T curve can be constructed. Hence from relatively simple and readily available information, such as the variation of viscosity with temperature, the heat of fusion, the melting point, etc., the cooling rate required to form a glass of a given material may readily be estimated.

The details of this treatment are presented in Ref. 1 in the list of publications under the grant.

II. EFFECTS OF NUCLEATING HETEROGENEITIES ON GLASS FORMATION

In any satisfactory discussion of glass formation, attention must be directed to the effects of nucleating heterogeneities, since these can give rise to the initial formation of crystals at relatively modest undercoolings. The effects of such heterogeneities have been explored during the present reporting period using the familiar model of a spherical cap nucleus. In employing this model, one needs to estimate the number of nucleating heterogeneities per unit volume characterized by a given contact angle θ. The total number of nucleating heterogeneities has been estimated as follows: Experiments on a variety of materials have indicated that division of a sample into droplets having sizes in the range of 10 microns in diameter is sufficient to ensure that most droplets (perhaps 99 pct.) do not contain a nucleating heterogeneity. For many materials, division into somewhat larger particles is sufficient. This technique has been widely used to study homogeneous nucleation; but the results can also be used to estimate a density of nucleating particles in the range of 10^9 cm^{-3}. Using this value together with an assumed heterogeneity size of 500 $\mathring{A}$, one obtains the total area of nucleating surface per unit volume.

The nucleation rate appropriate for constructing the TTT curves is then obtained using the standard treatment of heterogeneous nucleation:

$$I_V^s = A_V N_s^\circ \nu \exp - \frac{\Delta G^* f(\theta)}{kT} \qquad (9)$$

where A_V is the area of nucleating substrate per unit volume characterized by contact angle θ, N_s° is the number of molecules per unit area of

substrate, ν is the frequency factor for transport at the nucleus-liquid interface, ΔG^* is the free energy of forming the homogeneous critical nucleus, and

$$f(\theta) = \frac{(2 + \cos\theta)(1 - \cos\theta)^2}{4} \qquad (10)$$

The effect of the contact angle of nucleating heterogeneities on glass formation has then been evaluated by calculating TTT curves for different θ's. Such calculations have been carried out during the present reporting period. Typical results, for $Na_2O.2SiO_2$, are shown in Ref. 29, where ΔG^* has been taken as 50 kT at an undercooling relative to the liquidus, ΔT_r, of 0.2. As seen there, heterogeneities characterized by modest contact angles ($\theta \leq 80°$) can have a pronounced effect on glass-forming ability, while heterogeneities characterized by large contact angles ($\theta \geq 120°$) have a negligible effect.

Similar calculations have been carried out for a variety of materials--including simple oxides, metals, organics and water in addition to a number of lunar compositions--which indicate that nucleating heterogeneities with $\theta > 90$-$100°$ quite generally have a negligible effect on glass-forming ability. The results are typified by the comparison (Table 1) between the critical cooling rates estimated assuming only homogeneous nucleation and those estimated with the indicated density of heterogeneities all characterized by a contact angle of 80°. These results had not been predicted in advance, since all heterogeneities characterized by $\theta < 180°$ will lead to crystal nucleation at temperatures above that of homogeneous nucleation. Apparently, however, heterogeneities with $\theta > 90$-$100°$ do not lead to crystal formation at high enough temperatures

(relative to that of homogeneous nucleation) to affect the cooling rates needed to form glasses.

The effects on glass formation of changes in the barrier to nucleation are also shown in Table 1, where critical cooling rates are compared for barriers to homogeneous nucleation at $\Delta T_r = 0.2$ of 50 kT and 60 kT. As seen there, these effects can also be substantial. As indicated above, when the calculated rates for the lunar compositions are compared with experience in the laboratory, the difficulty of forming glasses is generally overestimated when ΔG^* is taken as 50 kT at $\Delta T_r = 0.2$. That is, the calculated cooling rates, even neglecting nucleating heterogeneities, are consistently too high. Reasonable agreement between calculated rates and laboratory experience on the lunar samples can be obtained by taking somewhat larger values for ΔG^* (in the range of 60-65 kT at $\Delta T_r = 0.2$ when only homogeneous nucleation is considered). Introduction of a sizable number of even reasonably potent nucleating heterogeneities would, however, increase the required barrier well above the range previously observed. It seems likely, therefore, that the lunar samples are characterized by an effective absence of potent nucleating heterogeneities ($40° < \theta < 80°$). As indicated above, heterogeneities with larger contact angles would have little effect on the glass-forming tendencies of the materials.

The effective absence of potent nucleating heterogeneities--and perhaps of all nucleating heterogeneities--may be associated with a number of factors. First, the lunar compositions are excellent solvents for refractory oxides and should dissolve such heterogeneities more effectively than the materials investigated in previous nucleation studies.

Table I

Estimated Cooling Rates for Glass Formation

Material	dT/dt (K sec^{-1}) homogen. nucl. $\Delta G^*=50$ kT @ $\Delta T_r=0.2$	dT/dt (K sec^{-1}) heterogen. nucl., $\theta=80°$ $\Delta G^*=50$ kT @ $\Delta T_r=0.2$	dT/dt (K sec^{-1}) homogen. nucl. $\Delta G^*=60$ kT @ $\Delta T_r=0.2$
$Na_2O \cdot 2SiO_2$	4.8	46	0.6
GeO_2	1.2	4.3	0.2
SiO_2	7×10^{-4}	6×10^{-3}	9×10^{-5}
Salol	1.4	220	1.7
Metal	1×10^{10}	2×10^{10}	2×10^{9}
H_2O	1×10^{7}	3×10^{7}	2×10^{6}
Apollo 15 green glass	4×10^{4}	7×10^{4}	7×10^{3}
Lunar Composition 15418	1×10^{4}	4×10^{4}	2×10^{3}
Lunar Composition 65016	7×10^{3}	1×10^{4}	1×10^{3}
Lunar Composition 60095	4×10^{3}	1×10^{4}	600

Second, the lunar materials existed for long times at high temperatures in the molten state, which also favors dissolution. Third, the lunar atmosphere may well be more free of heterogeneities than typical laboratory atmospheres on earth. Finally, the lunar atmosphere is free of water and should therefore eliminate surface nucleation associated with very thin water-rich surface layers, such as are often encountered in laboratory experiments on earth.

III. GLASS FORMATION UNDER CONTINUOUS COOLING CONDITIONS

In the previous kinetic treatment of glass formation based on TTT curves, the critical cooling rate required to just-avoid a given fraction crystallized was approximated by the relation:

$$\left(\frac{dT}{dt}\right)_c \approx \frac{\Delta T_N}{\tau_N} \qquad (3)$$

where $\Delta T_N = T_E - T_N$, T_N is the temperature of the nose of the TTT curve, and τ_N is the time at the nose.

It was recognized, however, that this relation overestimates the critical cooling rate since it implicitly assumes that the crystallization kinetics over the full range of temperature between the melting point and the nose of the TTT curve are as rapid as at the temperature of the nose. More realistic estimates of the cooling rates can be obtained by the construction of continuous cooling (CT) curves for the fractions crystallized of interest. These curves can be constructed from the corresponding isothermal TTT curves following the approach of Grange and Kiefer, an approach which has been elaborated and applied to the problem of glass formation under this grant.

The conversion from TTT curves to CT curves appropriate for continuous cooling under constant cooling rate conditions is illustrated by the results shown in Ref. 29. As seen there, the curves describing crystallization during continuous cooling indicate the formation of a given degree of crystallinity at lower temperatures and longer times than suggested by cursory examination of the TTT curves or use of Eqn. (3).

As an example, from CT curves, the critical cooling rate required to form a glass of the 70019 composition, and avoid the just-detectable degree of crystallinity of 10^{-6}, is estimated as about 4 K min^{-1}. For comparison, the critical cooling rate required to make a glass of this composition is estimated from Eqn. (3) as about 30 K min^{-1}.

This analysis has been applied to a sizable number of materials, including a variety of lunar compositions, a number of simple silicates, several organics and even metal alloys. The results, in general, are in close accord with experience.

IV. CRYSTALLIZATION STATISTICS

A complementary approach to the problem of glass formation was developed under the grant, which contains essentially complete statistical information about the state of crystallinity in a body. This approach is based upon introducing a "crystal density function" $\psi(\vec{r},t,R)$, such that the number dn of crystals in the volume dv at $\vec{r}$ having a radius between R and R+dR at time t is given by

$$dn = \psi(\vec{r},t,R)\, dv\, dR \qquad (11)$$

This function contains all of the basic statistical information about

the crystallinity of the system.

A crystal nucleating at a time $t_o<t$ has a radius at time t of

$$R(\vec{r},t,t_o) = \int_{t_o}^{t} u[T(\vec{r},t')]\, dt',\ R > 0 \qquad (12)$$

Here the temperature $T(\vec{r},t)$ is a specified function of position and time. For a given u(T) and $T(\vec{r},t)$, there exists a one-to-one correspondence between $R(\vec{r},t,t_o)$ and t_o. Thus, a crystal having radius R at position $\vec{r}$ and time t must have nucleated at a unique time $t_o<t$. Eqn. (12) therefore also serves to define implicitly a function $t_o(\vec{r},t,R)$, which for fixed $(\vec{r},t)$ is single valued in R.

The number dn of crystals in dv nucleating between t_o and t_o+dt_o is, by definition of the volume nucleation frequency $I_v(T)$,

$$dn = I_v[T(\vec{r},t_o)]\, dvdt_o \qquad (13)$$

To obtain ψ, we require the number of crystals having a radius between R and R+dR at the time $t>t_o$. This is most easily deduced formally by noting that the number of crystals nucleating during the finite time interval between t_1 and t_2 (with $t_1<t_2<t$) in the volume element dv is

$$dn_{12} = dv \int_{t_1}^{t_2} I_v\,[T(r,t_o)]\, dt_o \qquad (14)$$

From Eqn. (12), one obtains

$$\frac{\partial R}{\partial t_o} = -u\,[T(\vec{r},t_o)] \qquad (15)$$

Changing variables in Eqn. (14) with the aid of Eqn. (15), letting $R_1 \equiv R(\vec{r},t,t_2)$ and $R_2 \equiv R(\vec{r},t,t_1)$, and noting that $R_2>R_1$, one obtains

$$dN_{12} = dv \int_{R_1}^{R_2} \frac{I_v\{T[\vec{r},t_o(\vec{r},t,R)]\}}{u\{T[\vec{r},t_o(\vec{r},t,R)]\}} \tag{16}$$

Direct comparison with Eqn. (11) now shows that the integrand of Eqn. (16) is just $\psi(\vec{r},t,R)$:

$$\psi(\vec{r},t,R) = \frac{I_v\{T(\vec{r},t_o(\vec{r},t,R)]\}}{u\{T[\vec{r},t_o(\vec{r},t,R)]\}} \tag{17}$$

Other statistical distribution functions describing the state of crystallization of a sample can be either derived from (r,t,R) or obtained directly. First note that the largest crystal radius at (r,t) is given by

$$R_{max}(\vec{r},t) = \int_{t_o}^{t} u[T(r,t')]\, dt' \tag{18}$$

Then the number density of crystals at (r,t) is

$$D_N(\vec{r},t) = \int_0^{R_{max}} \psi(\vec{r},t,R)\, dR \tag{19a}$$

$$= \int_0^{t} I_v[T(\vec{r},t_o)]\, dt_o \tag{19b}$$

The volume fraction crystallized at (r,t) is

$$F_v(\vec{r},t) = \int_0^{R_{max}} \frac{4\pi}{3} R^3\, \psi(\vec{r},t,R)\, dR \tag{20a}$$

$$= \int_0^{t} \frac{4\pi}{3} R(\vec{r},t,t_o)^3\, I_v[T(\vec{r},t_o)]\, dt_o \tag{20b}$$

The average number density of crystals in the sample at time t is a simple volume average,

$$\bar{D}_N(t) = \frac{1}{V}\int_V D_N(\vec{r},t)\, d^3r \qquad (21)$$

Likewise, the volume fraction crystallized in the entire sample at time t is

$$F_v(t) = \frac{1}{V}\int_V F_v(\vec{r},t)\, d^3r \qquad (22)$$

For many purposes, the statistics are desired at a time long after crystallization has ceased (because the sample is cold). This case can be treated with the above analysis by using t^{cs}, the time at which crystallization essentially stopped, as one of the limits on the integrals over time, and the corresponding radius values as the limits on the integrals over R.

This analysis can be manipulated in various ways to obtain information about a specimen or a material. When u(T), $I_v(T)$ and $T(\vec{r},t)$ are known, a prediction of $\psi(\vec{r},t,R)$ is the most frequent objective. This may directly be used to assess the glass-forming characteristics of materials and the distributions of crystals in specimens having particular thermal histories. Where isothermal-transformation (T-T-T) diagrams are desired, they can be obtained directly from $T(\vec{r},t)$ and $F_v(\vec{r},t)$.

In addition to these direct calculations, various inversions are possible. As an example, if $I_v(T)$ and u(T) are known or can be calculated, and the final crystal density function is measured, then the temperature T_o at which a crystal of radius R nucleated can immediately be known. The more interesting example involves determining the thermal history

from post mortem crystallite statistics. In this case, the complete specification of the number of crystallites and their size distribution can be determined as a function of position by laboratory examination of samples. The isothermal nucleation and growth kinetics can also be determined by laboratory experiments; and the combination of such data with the results of the present analysis permits much information to be deduced about the thermal histories of the samples.

A further application of the analysis is the evaluation of the relative importance of various distributions of nucleating heterogeneities in affecting glass formation. Such an evaluation can be carried out for different viscosity-temperature relations and for various thermal histories, and should indicate the conditions under which different types of heterogeneities are critical to the formation of glasses.

It should be noted that neither the analysis nor the manipulations involved in the above applications involves explicit use of the position vector $\vec{r}$. The vector $\vec{r}$ merely serves as a label for the volume element under consideration, and the statistical treatment must be applied to each element separately. One consequence of this is that the thermal history of a small specimen which was originally part of a larger body can be determined independently of the availability of the original body.

This treatment is presented in detail in Ref. 13.

V. KINETICS OF CRYSTAL NUCLEATION

Since the greatest uncertainty in the treatment of glass formation lies in the evaluation of the nucleation frequency, attention was directed to measuring the kinetics of crystal nucleation over a wide range of temperature. The first material chosen for study in this regard was lunar composition 70019. As given in Ref. 31, the frequency of crystal nucleation for this material varies with temperature in a way which is predicted by the classical theory of homogeneous nucleation. This is shown by constructing a plot of $\ell n\ (I_v \eta)$ vs. $1/T_r^3 \Delta T_r^2$. Here I_v is the nucleation rate per unit volume; η is the viscosity; $T_r = T/T_E$, $\Delta T_r = \Delta T/T_E$, T_E is the liquidus temperature, and ΔT is the undercooling.

According to classical nucleation theory, the $\ell n(I_v \eta)$ vs. $1/T_r^3 \Delta T_r^2$ relation should be a straight line of negative slope; and such a straight line is indicated by the data on the 70019 material, which cover more than 10 orders of magnitude in $I_v \eta$. The slope of the least squares line through the data indicates a nucleation barrier of about 55 kT at $\Delta T_r = 0.2$ and the intercept at $1/T_r^3 \Delta T_r^2 = 0$ corresponds to a value of 5×10^{33} cm^{-3} sec^{-1} poise. The latter value is in excellent agreement with the value expected from the classical theory of homogeneous nucleation (about 10^{32} cm^{-3} sec^{-1} poise).

The agreement between experimental data and the predictions of classical nucleation theory, even in the pre-exponential factor, is remarkable. It indicates that homogeneous nucleation represents the dominant contribution to the formation of crystals, at least over the range of undercooling covered by the investigation (250C - 400C). In the range of large volume fractions crystallized, heterogeneous

nucleation on the crystals which originally formed by homogeneous nucleation may also be significant; and primary heterogeneous nucleation may well be important in the range of small undercoolings. The magnitude of the barrier to crystal nucleation indicated by the data, about 55 kT at $\Delta T_r = 0.2$, is in the range of values expected on the basis of the glass-forming abilities of a variety of lunar compositions.

More generally, the results of the study--in confirming the applicability of classical nucleation theory for describing the rate of crystal formation in a complex lunar composition, as well as the close agreement between growth rate data on synthetic and natural lunar samples (see above)--lend confidence to the use of the kinetic analysis in elucidating the thermal histories of glass-containing lunar samples.

VI. DIFFUSION CONTROLLED CRYSTAL GROWTH

In considering the crystallization of lunar compositions, one is in general concerned with processes involving large changes in composition. In many such cases, the rate of interface advance can be limited by transport processes in the liquid rather than by interface attachment kinetics. To explore the validity of this suggestion, an investigation was undertaken of crystallization under conditions of diffusion control. The treatment of such crystallization has importance for a variety of industrial processes as well as for several areas of geology.

Experimental data were obtained for a number of compositions in the simple analogue system, K_2O-SiO_2. At all temperatures of growth the interface morphology was dendritic in form, and the growth rate was independent of time. The variation of growth rate with temperature for

the 0.10 K_2O - 0.90 SiO_2 material is shown in Ref. 27. In describing these data, use was previously made of a simple model in which the composition gradient at the interface is approximated by the difference in concentration between the interface and infinity divided by the effective boundary layer thickness, and the interface concentration is taken as the equilibrium (liquidus) concentration for the temperature of growth.

This simple model was found to describe reasonably well the crystallization kinetics of two of the compositions studied, including the 0.10 K_2O - 0.90 SiO_2 material. It was recognized, however, that the approximation to the interface gradient used in this model was highly simplified, and that this approximation limited significantly any physical understanding of the experimental results.

The development of an improved theoretical description of dendrites growing in the presence of neighboring dendrites was also carried out under the grant. The results of this analysis are presented in Ref. 25.

The model advanced in this paper takes account of the effect of overlapping diffusion fields from neighboring dendrites by a modification of the approach used by Jackson and Hunt in their classic analysis of rod eutectic growth. The analysis leads to an expression of the growth rate in terms of physically measurable quantities which depends upon the form of the concentration gradient ahead of the interface. For the simplest case, in which the concentration gradient decreases as a step function at the radius of the dendrite (see Fig. 2a in Ref. 25), the following expression is obtained for the growth rate:

$$u = \frac{D}{2rS(a)}\left[\frac{(C_E - C_o)}{(C_E - C_S)} - a^2\right] \tag{23}$$

where we have defined

$$S(a) = \sum_{n=1}^{\infty} \frac{J_1(\lambda_n a)}{[\lambda_n J_o(\lambda_n)]^2} \tag{24}$$

where u is the growth rate, D is the diffusion coefficient, C_E is the interface concentration, assumed equal to the equilibrium liduidus concentration; C_S is the composition of the solid; C_o is the concentration of the bulk liquid; a = r/R, where r is the radius of the dendrite and R is the radius of the cylinder of symmetry around the dendrite across which no diffusive flux occurs; J_o is a Bessel function of the first kind of order zero; J_1 is a Bessel function of order unity; and λ_n are the roots of $J_1(\lambda_n) = 0$.

Using values of C_E from the metastable cristobalite liquids of the phase diagram and data on D of May and Wollast, Eqn. (11) has been used to calculate growth rates. The results are shown as u_1 in Ref. 25; in that figure u_E represents the experimental data. The agreement is surprisingly good, considering the simplicity of the model: u_1 is within a factor of 3.9 of the experimentally determined growth rates under all conditions; and in most cases, the agreement is within about a factor of 2.

Two other choices for the concentration gradient have been tried. The forms of the assumed concentration gradients at the plane of the dendrite tip (z = 0) are shown in Fig. 2 of Ref. 25; in that figure we have defined $A \equiv (u/D)(C_S - C_E)$. The broad distribution in Fig. 2b

leads to the calculated growth rate u_2; the narrow distribution in Fig. 2c leads to u_3. The calculated and observed growth rates are compared in Fig. 5. At temperatures below about 1050 C, u_1 is seen to be an improvement over u_3, and u_2 is an improvement over u_1.

These results suggest that the concentration of solute near the tip of the dendrite is higher than for an isolated dendrite. The buildup of solute around the tip of the dendrite leads to a diffusion flux away from the array of dendrites into the bulk liquid. The lateral flux from the parabolic surface of the dendrite is inhibited by the lateral flux from neighboring dendrites. Therefore a greater flux in the direction of the bulk liquid is required, when the dendrite is not isolated, to carry away the rejected solute. When such a flux is built into the model, the calculated growth rates shift from those expected for an isolated dendrite (u_3) toward the experimental values.

As indicated above, the results of this analysis should have wide application in describing the crystallization of lunar compositions as well as many commercial glass-forming systems.

VII. CRYSTALLIZATION OF LUNAR COMPOSITIONS

The crystallization behavior of a wide range of lunar compositions was determined under the grant. In all cases, data were obtained over a wide range of temperature, typically 300-400°C. The compositions investigated include Lunar Compositions 14259 and 14310 (Ref. 2), 15555 (Ref. 6 and Ref. 9); Apollo 15 Green Glass, 15418, 65016 and 60095 (Ref. 15); 70019 and 79155 (Ref. 24); 15286 and 15498 (Ref. 30); 67975 (Ref. 36);glassy intrusion in 15286 (Ref. 37); and low Ti, low Mg

mare basalt composition and highland basalt composition (Ref. 42).

The data obtained on the various compositions are presented in the indicated papers, as are specific data on the liquidus temperatures of the specific compositions. In all cases, the materials crystallize with a considerable change in composition; in all cases, growth is expected to take place by a diffusion controlled process; but in all cases, the growth rate was found to be independent of time. The lack of dependence of the growth rate on time provides evidence for a coupled diffusion controlled process of the type analyzed theoretically and discussed above.

VIII. CRYSTALLIZATION BETWEEN SOLIDUS AND LIQUIDUS

It was noted during the period of support by the grant that the basic assumption of the standard treatment of solute redistribution during solidification was inappropriate for many solidification situations, including those which apply for glass-forming lunar compositions. In particular, the standard treatment is based on the assumption that the concentration of solute in the solid at the interface is a constant fraction of the concentration in the liquid at the interface. This assumption is applicable to cases where a solidifying solution is translated through a first thermal environment, with the rate of advance of the interface being limited by heat flow. While such conditions often maintain for the unidirectional solidification of metals, they represent poorly the typical crystallization experiments carried out in the laboratory on glass-forming materials or the crystallization of glass-forming compositions in the lunar environment.

A new analysis was carried out during the grant. This new analysis

is appropriate for situations where the advance of the interface is limited by attachment kinetics which produce an approximately constant growth velocity under isothermal conditions. The analysis is based upon the assumption of local equilibrium between solid and liquid at the interface at a given temperature. This assumption may be stated in terms of the familiar free energy vs. composition relations for the crystal and liquid solutions, as follows: the composition C_s of the crystal in equilibrium with liquid of composition C_L is given by the tangent from the liquid free energy curve at C_L to the crystal free energy curve.

This new condition stands in sharp contrast to that used in previous analyses (where C_s was taken as a constant fraction of C_L). With the new condition, C_s decreases with increasing C_L, approaching the limiting value C_{se} and C_L approaches C_{Le}. Here C_{se} and C_{Le} are, respectively, the solidus and liquidus compositions at the temperature of crystallization. An immediate consequence of the fact that C_s does not approach the average composition C_o is that there can be no steady state of the type anticipated by the previous analysis.

The differences between the two analyses are shown in Figs. 4a and 4b from Ref. 11 which depict the composition in the crystal and liquid phases as a function of the distance crystallized. Figure 4a depicts the standard analysis in which the solid composition at the interface increases from kC_o toward C_o as the liquid composition increases from C_o to C_o/k. Here k is the distribution coefficient at the interface ($k = C_s/C_L$). Figure 4b depicts the new analysis in which the solid composition decreases toward C_{se} as the liquid composition increases from C_o toward C_{Le}.

The implications of this analysis for t'.e question of zoning are obvious; and the importance of elucidating the appropriate interface condition is clearly indicated. Such work is being carried out at the present time.

IX. CRYSTALLIZATION ON REHEATING A GLASS

The technique of quenching a liquid to a glass and observing crystallization on subsequent reheating is widely used to evaluate the glass-forming abilities of different materials. The stability of glasses against subsequent reheating is also of importance in the disposal of radioactive wastes (see discussion in preceding section) and in understanding the preservation of glasses in the lunar environment. During the present period of the grant, an analysis has been developed to describe crystallization on reheating a glass at an arbitrary rate, R, which glass was originally formed by cooling at a rate, R_2. Here R_2 may be the same as or different from R_1.

In many laboratory experiments concerned with glass formation, the temperature of maximum crystallization rate, T_{cr}, is determined by differential thermal analysis (DTA) or differential scanning calorimetry (DSC). Hruby formulated a parameter

$$K_{gl} = \frac{T_{cr}-T_g}{T_E-T_{cr}} \tag{25}$$

as a measure of glass-forming ability. This parameter provides a convenient reference for describing the process of crystallization on reheating a glass. The treatment used to describe this process is outlined in Ref. 45. In this treatment, one considers a crystal

nucleating at a time t_o ($t_o < t$), which has a radius at time t of

$$R(t,t_o) = \int_{t_o}^{t} u[T(t')]dt' + R^*[T(t_o)] \tag{26}$$

Here R^* is the radius of the critical nucleus, which can be expressed from classical nucleation theory as:

$$R^* \approx \frac{0.5V_M^{1/3} T_E^2}{N_o^{1/3} \Delta T \; T} \tag{27}$$

where V_M is the molar volume and N_o is Avogadro's number.

The state of crystallinity in a body is described in terms of the crystal distribution function ψ, introduced in Ref. 13 and described above. In describing devitrification on reheating a glass in terms of this formalism, it is assumed that if at any time and temperature the crystallite is smaller than the critical size corresponding to that temperature, it will melt completely and will not be included in any future calculations of the crystal distributions; that is,

$$\psi(t,t_o) = 0 \tag{28}$$

when $R(t',t_o) < R^*(t')$ for some t' on (t_o,t). There will be a range of $R(t,t_o)$ for which $R(t',t_o) > R^*(t')$, and the number of crystallites in that range can be calculated.

Taking account of the number of crystals which nucleate during the time interval between t_1 and t_2, one obtains an expression for the crystal distribution function:

$$\psi = \frac{I_v\{T[t_o(t,R)]\}}{u\{T(t_o(t,R))]\} - \dfrac{dR^*[t_o(t,R)]}{dt_o(t,R)}} \tag{29}$$

The inclusion of R^* in the expression for the crystallite size is significant when calculating the volume fraction crystallized. When the temperature is cycled below the glass transition, where the growth rate is essentially zero but dR^*/dt_o is not, as well as when a sample is cooled below and reheated above the glass transition, the expressions of Eqns. (26) - (29) are necessary to obtain reliable results.

The volume fraction crystallized has been calculated for several materials with thermal histories that include cooling from the melt to a temperature below the glass transition temperature and subsequent reheating until crystallization takes place. The growth rate and viscosity for each material were determined experimentally. The nucleation barrier was varied in the range suggested by the results of previous workers:

$$I_v = N_v^o \nu \exp - \frac{.02048B\ T_E^{\ 5}}{(\Delta T)^2 T^3} \qquad (30)$$

where N_v^o is the number of molecules per unit volume; ν is the frequency of transport at the nucleus-matrix interface (which is inversely related to the viscosity); and B = 40-75, which corresponds to a nucleation barrier of BkT at a relative undercooling (ΔT_r) of 0.2. At every step in the integration, the crystallite sizes were compared with the critical nucleus size for that temperature, and any crystallites that were smaller than the critical size were no longer included in calculations of the volume fraction crystallized.

The temperature range in which the greatest amount of crystallization takes place is taken as the crystallization temperature, T_{cr}. The temperature of crystallization is found to depend strongly on the heating rate, and also upon the cooling rate used to form the glass. The results

indicate that not all glasses are in the same state at the glass transition, but the state depends upon the cooling rate at which the glass was formed. It has also been found that the magnitude of the nucleation barrier has a pronounced effect on the crystallization temperature. This is shown in Ref. 45 for anorthite. From this figure, it is clear that one can estimate the nucleation barrier from the temperature of the crystallization peak as a function of heating rate.

To provide a test of the new analysis, experimental data were obtained on the matrix composition of lunar breccia 67975 and on anorthite. In the case of the breccia, direct measurements of the nucleation barrier were carried out (see below). With these data, together with previous measurements of the growth rate and viscosity, CT curves corresponding to a just-detectable degree of crystallinity ($V_c/V = 10^{-6}$) were constructed. From these curves, the critical cooling rate required to form this material as a glass is estimated as about 1-2°C min^{-1}. To verify this estimate and to test the predictive power of the kinetic analysis, samples of the 67975 matrix composition were cooled at a variety of rates under controlled atmosphere conditions (the same as used in the nucleation and crystal growth studies) to determine the critical cooling rate for glass formation. It was found that sensibly crystalline bodies were produced at a cooling rate of 3°C min^{-1}. This indicates a remarkable agreement between the predictions of the kinetic analysis and experimental data.

As a further test of the kinetic approach and as a direct attempt at verification of the new treatment of crystallization behavior on reheating a glass, samples of the 67975 composition were cooled rapidly to the glassy state and were subsequently reheated at a number of rates

in a differential thermal analyzer (DTA). Quite good agreement was found between the predicted and experimental values of T_{cr} as well as between the predicted and measured dependence of T_{cr} on heating rate.

X. TEMPERATURE DISTRIBUTIONS DURING CRYSTALLIZATION

It is well recognized that the crystallization rate of a given material will in general be limited by one of three processes:

1. interface attachment kinetics;
2. diffusion of particular species to or from the interface; or
3. heat flow.

The first limitation is illustrated by the growth of crystals from melts of high viscosity, the second by flux growth, and the third by growth at high rates from melts of low viscosity.

In the present section, we shall discuss an analysis which was carried out under the grant of heat flow during crystallization and of the transition from interface-controlled growth to heat-flow-controlled growth. The results are useful for understanding and predicting the crystallization behavior of many materials.

The analysis has specifically been concerned with the temperature distribution in a crystal-liquid system which is crystallizing at constant velocity, v_o, with a planar interface. For simplicity, the thermal properties of liquid and crystal have been taken as identical and a system of infinite extent has been assumed. The effects of finite specimen size are then considered separately. The results of the analysis should be directly applicable to crystallization in glass-forming systems where the assumed constant growth rate is provided by the kinetics

of the interface process.

Direct analytical expressions have been obtained for the temperature at any position and time in both the liquid and crystal phases. The temperature profile in the liquid in front of the moving interface approaches a steady state at large times. That is, letting $\zeta = x - v_o t$ be a spatial coordinate with respect to the moving interface (the interface is at $\zeta=0$), one expects that for any $\zeta>0$, $T^L(\zeta,t)$ becomes constant in time as $t\to\infty$. The analogy in this case with the corresponding solute rejection problem is obvious. $T^L(\zeta,t)$ is, of course, the temperature in the liquid at position ζ at time t.

Such a steady state form for the temperature profile is not, however, expected for the solid. Even at large times, one will always be able to find sufficiently small $\zeta<0$ (i.e., sufficiently large $|\zeta|$) such that $dT^S(\zeta,t)/dt$ is finite. Here $T^S(\zeta,t)$ is the temperature in the solid at ζ and t. The difference between the two cases is as follows: in the liquid the interface is moving in the direction of the flux, and eventually the flux is small enough that the two move together; but in the solid, the flux and the interface move in opposite directions, and the two can never move together.

The results of the analysis have been applied to representative materials in three classes: glass-forming oxides ($Na_2O.2SiO_2$), glass-forming organics (α-phenyl o-cresol) and metals (Sn). For the oxide glass-former under a wide range of experimental conditions, the interface temperature should depart negligibly from the furnace temperature. Crystallization kinetics corresponding to interface-controlled growth would therefore be observed. For the organic glass-former, the

interface temperature should correspond closely to the bath temperature for thin specimens (and hence observed growth rates should represent interface-controlled growth); while for specimens of modest size appreciable interface heating is predicted, and a transition from interface-controlled growth to heat flow-controlled growth should be observable. For the metal, the interface temperature should very quickly heat to the vicinity of the melting point (in growth times of the order of 50 microseconds or extents of growth of the order of 6 microns); and heat flow-controlled growth would be expected quite early in the crystallization process.

The infinite-system analysis indicates an ultimate interface heating, β, given by

$$\beta = L/C \qquad (31)$$

where L is the latent heat of fusion and C is the specific heat. In addition to β, the temperature distribution depends upon the distances from the interface, ζ, and upon the extent of growth, $v_o t$. These two distances are scaled in the temperature expression by the parameter α in the dimensionless quantities $\zeta=\zeta/2\alpha$ and $u=v_o t/4\alpha$. Here $\alpha = \kappa/v_o$, where κ is the thermal diffusivity. Thus the spatial extent of the temperature distribution will increase with increasing thermal diffusivity and with decreasing growth rate, but a greater extent of growth will be required for a given interface heating to be obtained.

This analysis is described in detail in Ref. 8,

XI. CRYSTALLIZATION OF ANORTHITE AND ANORTHITE-ALBITE COMPOSITIONS

The kinetics of crystallization of anorthite and 3 anorthite-albite compositions ($An_{75}Ab_{25}$, $An_{50}Ab_{50}$ and $An_{20}Ab_{80}$) have been obtained over wide ranges of temperature (400 Centigrade degrees), from somewhat below the liquidus to below the solidus. The work on the An-Ab materials was carried out in collaboration with Professor J. Kirkpatrick (now with the University of Illinois) and Professor J. F. Hays of Harvard, who measured the kinetics of crystallization in the range of temperature near the liquidus on samples supplied from our melts.

The results obtained on anorthite are presented in Ref. 18 and those on the three An-Ab compositions in Ref. 47. As indicated in Ref. 47, the growth rate at any temperature (or at any undercooling below the respective liquidus temperatures), as well as the maximum growth rate for a given composition, decrease with increasing Ab content. These variations can all be related to a decrease in the molecular mobility at a given temperature, and a decrease in the liquidus temperature with increasing Ab content.

The observed changes in crystal morphology with increasing undercooling--euhedral to skeletal to dendritic, and finally to spherulitic or fibrillar--are the same as those observed by Lofgren for plagioclase crystals grown from water saturated compositions in the system anorthite-albite-H_2O at about 6 kb.

The observed independence of the growth rates on time is consistent with either diffusion-controlled or interface-controlled growth. In light of the sizable redistribution of material required for growth of

these compositions, diffusion-controlled growth seems a priori likely. For growth at undercoolings greater than about 40°C, where skeletal, dendritic, spherulitic or fibrillar morphologies are observed, the crystallization process is almost certainly diffusion-controlled.

Even at very large undercoolings, where the overall crystal morphology is spherulitic or fibrillar, the crystals may be locally faceted (Figs. 2-8 of Ref. 47). This is in accord with the locally faceted morphologies observed by Scherer and Uhlmann for crystals growing at large undercoolings from incongruently-melting compositions in the K_2O-SiO_2 and Na_2O-SiO_2 systems. This local faceting indicates that even when the overall growth rate is controlled by diffusion in the melt, the anisotropy of the interface attachment kinetics can still be important on a local scale.

The nature of the crystallization process at small undercoolings has not been established unequivocally. The faceted (euhedral) morphology coupled with the time-independent growth rates could be taken as evidence of interface-controlled growth, with the morphological transition observed at undercoolings of about 40-50°C representing a transition of diffusion-controlled growth. The alternative suggestion, that the growth is diffusion-controlled even at small undercoolings, receives support from the observations of time-dependent growth rates as crystals approached one another and from observations of convective motion in the melt (with the time-independent growth reflecting an essentially unchanging diffusion boundary layer at the interface). Further experimentation--e.g., the determination of the presence or absence

of a diffusion boundary layer around the crystals--is required to resolve the issue.

The agreement between the data obtained using the two experimental techniques indicates that the growth rate does not depend on whether the sample was first quenched to a glass and then heated to the crystallization temperature or was cooled directly to the crystallization temperature from above the liquidus. This implies that for these compositions and temperatures the structural state of the liquid reaches equilibrium rapidly relative to the time scale of crystallization.

XII. EFFECTS OF IRON OXIDATION STATE ON VISCOSITY

The oxidation state of iron is expected to affect significantly many properties of iron-rich materials; and a knowledge and control of such effects is important in a sizable number of applications ranging from terrestrial geology to the fabrication of fiber optic waveguides.

In the area of rheology, almost nothing has been known about the effects on liquid viscosity of changing Fe^{2+}/Fe^{3+} concentration ratios, for a given total iron content. To investigate such effects, lunar composition 15555 seemed highly desirable, since its high iron content (22 wt. pct) would make readily apparent the role of oxidation state affecting liquid viscosity.

Such a study has been carried out during the present contract period. The synthetic material having the composition of lunar sample 15555 was prepared and melted under conditions of different oxygen activity. Percentages of total iron in the Fe^{2+} state were determined by chemical analysis, both after melting and after the determination

of viscosity.

To avoid changes in the iron oxidation state during the viscosity measurements, attention was directed to the range of high viscosities. The data were obtained with the bending beam instrument used in other investigations of lunar compositions. In all cases, the Fe^{2+}/Fe^{3+} concentration ratios after the viscosity measurements were unchanged from values obtained prior to the viscosity measurements. The percentages of total iron in the Fe^{2+} state in the three sets of samples studied in detail were: 94%, 76% and 20%.

The results of the viscosity determinations are shown in Ref. 12. As noted there, a change in the Fe^{2+}/total Fe ratio from 0.94 to 0.76 has a negligible effect on the viscosity over the measured range of temperature. In contrast, further oxidation to a Fe^{2+}/total Fe ratio of 0.20 has a pronounced effect in increasing the viscosity while leaving relatively unchanged the form of the variation of viscosity with temperature.

An electron microscope study was carried out to investigate the possible occurrence of liquid-liquid immiscibility (which could serve to increase the viscosity) in the most oxidized sample. The study indicated the absence of observable submicrostructure in the specimen glass, and suggests that immiscibility was not a significant problem for the oxidized composition.

The observed variation of viscosity with iron oxidation state was not anticipated. The change from Fe^{2+} to Fe^{3+} is expected to be accompanied by a change in the iron coordination from octahedral to tetrahedral. Such a change, together with the concomitant change in valence and local cohesion, would in turn be expected to result in

an increase in the viscosity of the liquid. For a continuous change in the fraction of tetrahedrally coordinated iron with changing oxidation state, together with the accompanying continuous change in local cohesion, the increase in viscosity should also be continuous. The present results indicate, however, a viscosity for the material with a Fe^{2+}/total Fe ratio of 0.76 which is effectively identical to that of the material with a ratio of 0.94, and then a dramatic increase in viscosity for the material with a ratio of 0.20.

A number of possibilities may be suggested to account for the observed behavior. These include the effects of a coupling between iron ions in the glass and the role of local charge compensation by other modifying cations. The details of these suggestions are rather lengthy for the present report, and are presented in Ref. 12.

It should be emphasized, however, that these suggestions are highly tentative; and further work on structurally simple glasses containing large concentrations of iron, with small increments in the Fe^{2+}/Fe^{3+} ratio, seems indicated.

Although incidental to the main thrust of the viscous flow study, it was noted that the samples containing about 80 pct. of the iron in the Fe^{3+} state exhibited internal nucleation of crystals to a sizable extent, while the samples containing large concentrations of ferrous iron exhibited only surface nucleation. The greatly enhanced internal nucleation in samples containing large concentrations of ferric iron is not satisfactorily understood at the present time. It apparently

does not involve liquid-liquid immiscibility as an essential feature, but may depend critically upon a pairing of the tetrahedrally-coordinated Fe^{3+} in highly regular configurations. In any case, the observations have potentially great significance for the controlled crystallization of glass-ceramic bodies, which depends critically upon internal nucleation of crystals in glass-forming liquids.

XIII. DIFFUSIVE CREEP AND VISCOUS FLOW

Attention was directed during the grant to the relation between diffusive creep and viscous flow. This was occasioned by previous treatments by others of phenomena such as convection in the interior of the moon in terms of Newtonian hydrodynamics. Since the interior of the moon is, with the possible exception of a small molten core, by no means a liquid, it seemed desirable to investigate the validity of using a hydrodynamic formalism to describe a phenomenon which might better be represented as a diffusive creep. The following paragraphs represent a summary of our consideration of the problem, which is presented in detail in Ref. 14.

It should be recognized at the outset that the differences among the types of flow are important not only in calculating deformation rates in general states of stress, but also in discussing theories of viscosity. In the latter regard, several notable theories compute directly a self diffusivity (D) of the material and deduce the viscosity (η) from an assumed relation between D and η.

The familiar relations between D and η result from two classes of analyses. The first is essentially molecular, relating the motion of

an atom to the viscosity of the liquid. This approach, represented by the Stokes-Einstein relation, can provide a valid connection between the diffusivity and the viscosity of a liquid. The existence of such a connection does not, however, imply that there is a diffusive mechanism for viscous flow, or that there is a connection between macroscopic diffusive and viscous deformations. The theory relates self diffusivity to viscosity, not diffusive fluxes to viscous flows. The molecular theory provides no justification for inferring that diffusive fluxes can be represented as macroscopic flows satisfying the rheological equation of a Newtonian viscous liquid.

The second type of analysis which is used to obtain relations between D and η treats the macroscopic flow behavior as a diffusional process and as a viscous process, and equates the rates of flow to obtain the D-η relation (i.e., the theories attempt to relate directly the diffusive motion of individual molecules or vacancies to a viscosity). This approach is fraught with difficulties, since diffusive motions do not directly produce hydrodynamic shearing flows, and macroscopic stress fields do not directly induce individual molecular motions, except as a second order effect.

When comparing diffusional creep and creeping viscous flow, it is immediately noted that both are characterized by deformation rates proportional to the applied stress. The two processes are, however, distinct on both macroscopic and molecular scales. Consider first diffusional creep, the deformation of a body by volume diffusion of individual molecules or vacancies. In particular, consider vacancy diffusion in an otherwise perfect crystal lattice, recognizing that the

same arguments are applicable to amorphous materials. For small vacancy concentrations and concentration gradients, such as are anticipated in planetary interiors, the diffusion field is in steady state described by:

$$\nabla^2 (\mu_a - \mu_v) = 0 \tag{32}$$

and the atom fluxes produce a material velocity of

$$v = - \frac{D_a^*}{RT} \nabla(\mu_a - \mu_v) \tag{33}$$

Here D_a^* is the tracer diffusivity of the atoms, and μ_a and μ_v are respectively the chemical potentials of atoms and vacancies.

These expressions are not equivalent to those which describe the isothermal, incompressible flow of a Newtonian liquid: first, the continuity equation

$$\nabla \cdot v = 0 \tag{34}$$

Then the Navier-Stokes (momentum) equation, which for creeping viscous flow is the simple Stokes equation:

$$\nabla p = \eta \nabla^2 v \tag{35}$$

Here p is the pressure and η is the viscosity.

In addition to the basic expressions describing diffusive creep and creeping viscous flow being different, the boundary conditions are also different. Creeping viscous flows will therefore differ from diffusive creep flows: The velocity fields will almost always be different for identical boundary conditions; and for identical velocity fields, the boundary stresses will be different and the dissipations will be unequal.

To explore these differences, the capillarity-induced spheroidization by diffusive creep and creeping viscous flow of a nearly spherical body has been considered. The results, presented in Ref. 14, indicate clearly that the two treatments yield predictions which are by no means equivalent.

It was suggested, therefore, that the behavior of bodies in diffusive creep, such as the interior of the moon, should not be described by viscous flow equations.

XIV. HIGH TEMPERATURE FLOW BEHAVIOR OF GLASS-FORMING LIQUIDS, A FREE VOLUME INTERPRETATION

A number of theoretical models have been advanced to describe the viscous flow behavior of liquids. Notable among these are absolute rate theories, free volume theories, and excess entropy theories. It has been found in recent years that none of these models can satisfactorily describe flow behavior over the full range of measured viscosity. Significant differences are found in the flow behavior of various liquids, both within a given class of materials, such as inorganic oxide liquids, as well as between different classes of materials, such as inorganic oxides and simple organics.

In work carried out under the grant, it has been found that free volume theories provide a close description of the flow behavior of both inorganic oxide and simple organic liquids in the high temperature region. In the typical case, such models describe closely the measured variation of viscosity with temperature over the range between 10^{-2} and 10^{+4} poise. Even the pre-exponential factors determined experimentally

are close to those predicted by the theory.

In light of this remarkable agreement between theory and experiment, it is suggested that free volume theories be used to describe flow behavior in the high temperature region, rather than in the high viscosity region as the glass transition is approached. This suggestion stands in contrast with a number of previous developments, including the familiar Williams-Landel-Ferry relation. The suggestion is, however, in accord with the success of free volume theories in describing: (a) the results of molecular dynamics calculations of liquid transport; (b) the temperature dependence of the flow of fluid hydrocarbons; and (c) the temperature and pressure dependence of the flow of rare gas liquids. It also avoids the difficulties posed by the failure of such theories to describe the pressure dependence of the glass transition.

Use of the new high temperature parameters in the free volume model overestimates the difficulty of flow in the high viscosity region (above 10^4 poise). The fractional free volume at the point of departure of the experimental data from free volume predictions for both organic and inorganic liquids--including the results on anorthite described above--is approximately 0.015. In the high viscosity region, a second, easier flow process--perhaps involving transport over potential energy barriers--appears to become dominant.

With these findings, a new high-temperature relation has been suggested:

$$\eta \approx \frac{(MkT)^{1/2}}{a_o^2} \exp\left[\frac{0.25}{0.015 + \Delta\alpha(T-T_B)}\right] \qquad (36)$$

where a_o is the molecular size evaluated from density data, M is the molecular mass, $\Delta\alpha$ is the difference in volume thermal expansion coefficient between liquid and glass, and T_B is the low-temperature limit of applicability of the free volume model, corresponding to viscosities in the range of 10^4 poise.

The high-temperature flow data on all the lunar liquids investigated to date can be well represented by such a free volume model. In addition to this application, the suggestion that free volume theories be used to describe liquid flow in the fluid region, rather than in the region around the glass transition, has wide ranging implications in many other areas involving the flow and processing of liquids.

The results obtained in the area of volume representations of high temperature flow data are summarized in Ref. 7, which deals with the viscosity of liquid anorthite, as well as in Ref. 10, which deals with the general question of describing flow behavior with a free volume model.

XV. VISCOUS FLOW BEHAVIOR OF LUNAR COMPOSITIONS

The viscous flow behavior of sizable number of lunar compositions was determined under the grant. In all cases, the viscosity has been measured using a rotating-cylinder viscosimeter for the high-temperature range and a bending-beam viscosimeter for the range of high viscosity (as the glass transition is approached). For all lunar compositions, the samples were melted and tested under conditions of low oxygen activity to simulate the ferrous/ferric concentration ratios of the moon.

The lunar compositions whose flow behavior was investigated include: 14259 and 14310 (described in Ref. 2); 15418 (described in Ref. 4);

15555, 68502 and 74220 (described in Ref. 9); 60095, 65016 and the Apollo 15 green glass (described in Ref. 15); 70019 and 79155 (described in Ref. 24); 15286 (intrusion) and 15418 (described in Ref. 30); 67975 (described in Ref. 36); 15286, matrix (described in Ref. 37) and low Ti, low Mg mare basalt composition and highland basalt composition (described in Ref. 42).

For all of these materials appreciable curvature is noted in the overall log (viscosity) vs. $1/T_r$. In all cases, the high temperature data can be well represented by relations of the free volume form. The high temperature flow data on the lunar compositions are also in close agreement with predictions of the semi-empirical models of Shaw and Bottinga and Weill. In the low temperature, high viscosity region, pronounced variability is noted in the forms of the viscosity-temperature relations for the different compositions. A similar variability in form of the low-temperature flow data has been observed in other studies of both organic and inorganic liquids. The flow in this region seems likely to involve transport over potential barriers, but with a significant degree of cooperation.

XVI. THERMAL HISTORY OF ORANGE SOIL MATERIAL

The rate at which the orange soil material (lunar composition 74220) cooled through the region of its glass transition has been determined from scanning calorimetry studies. The salient results are summarized in Refs. 6 and 15.

The heat capacity vs. temperature relation for the lunar glass exhibited, at a heating rate of 20°K min^{-1}, a glassy heat capacity

which increases slightly with increasing temperature to values in the range of 0.24 cal gm^{-1} $°K^{-1}$ at temperatures of 840°-890°K. A dip is observed in the C_p vs T relation in the range about 910°K; this is followed by a rapid rise in heat capacity to liquid values of about 0.34 cal gm^{-1} $°K^{-1}$ at temperature of about 950°K.

Comparison heating runs were also carried out at 20°K min^{-1}, following cooling at 320°, 80° and 20°K min^{-1}. The results are shown in Ref. 6. The dip in the as-received curve indicates that the sample was initially cooled at a rate far exceeding 20°K min^{-1}. From the comparison curves, it appears that the original lunar material cooled at a rate somewhat in excess of 320°K min^{-1} (perhaps 400-500°K min^{-1}). This estimated cooling rate for the lunar material is consistent with observations of the flow and crystallization behavior of synthetic material of the same composition, which indicate that the lunar material cooled at a rate near the minimum required for glass formation. Because of its high fluidity at temperatures below the liquidus and its rapid crystallization kinetics, the 74220 composition cannot occur as a glass body on the moon of a size larger than the mm range; and even smaller upper limits on the size obtainable as a glass are suggested by calculations of cooling rates obtainable under radiant conditions.

XVII. BRECCIA FORMATION BY VISCOUS SINTERING

Clastic or fragmental breccias constitute an important type of rock returned from the lunar surface. Some workers have suggested that the welding of these lunar breccias took place by a shock lithification of unconsolidated material in the presence of relatively high dynamic shock

pressures. It has been noted, however, that there are some serious difficulties with the view of shock lithification as the general mechanism of clastic breccia formation; and our work was motivated by the suggestion, notably advanced by Simmonds, that the coherency of the breccias results from sintering of the fine grain matrix in a stress-free environment.

Our investigations in this area built upon previous work in our laboratory concerned with the crystallization behavior of representative lunar materials and the formation of lunar glasses. The approach uses combined information on crystallization and sintering kinetics under various conditions of continuous cooling. In particular, the approach is capable of providing clear insight into the thermal history of breccias which are not completely crystallized--i.e., breccias which are low-grade to medium-grade in Warner's classification. The view has been adopted that if a material crystallizes completely before significant sintering takes place, an unconsolidated powder or a friable material which is slightly welded at points of inter-particle contact will be produced; while if the matrix particles sinter appreciably before crystallization, largely amorphous breccias or breccias with varying degrees of crystallinity will result, depending upon the thermal history.

Our first approach to this problem was based upon treatments of crystallization and viscous sintering under isothermal conditions (Ref. 21). Crystallization kinetics were included by constructing time-temperature-transformation (TTT) curves corresponding to various degrees of crystallinity; and sintering kinetics were included by using the Frenkel treatment of viscous sintering to estimate the time required at a given temperature to obtain a significant degree of sintering. Using

these treatments in combination, it is possible to delineate regions in which bodies of different types will be formed. As shown in Ref. 21 for lunar composition 70019, amorphous breccias will be produced when there is sufficient time for the matrix material to sinter, but not sufficient time for it to develop a detectable degree of crystallinity. Breccias with partly or completely crystallized matrix material will result when the time is not only sufficient to produce a sintered matrix, but is also sufficient for various degrees of crystallinity to be developed. A largely uncompacted powder will be produced when the time is insufficient for the body to sinter or when the material crystallizes prior to the occurrence of significant sintering. As shown in Ref. 21, breccias with degrees of crystallinity between 0.1 and 0.5 will be formed under isothermal conditions only in a rather narrow range of temperature and time.

Recognizing that the clastic lunar breccias formed under various conditions of continuous cooling, the analysis was extended to describe crystallization and sintering under such conditions. In the case of crystallization, use has been made of continuous cooling (CT) curves corresponding to the degree of crystallinity observed in the matrix of the breccias. The CT curves are obtained from corresponding TTT curves following the approach discussed in Ref. 23. As in previous studies of crystallization and glass formation, the TTT curves are generally constructed from measured values of the crystal growth rate as a function of temperature together with calculated values of the nucleation frequency.

Sintering under continuous cooling conditions has been described by an analysis carried out under the grant (see discussion in the following

section). This analysis permits a determination of the minimum temperature at which the particles of the matrix material must have come in contact for various cooling conditions, including both linear and logarithmic cooling.

XVIII. VISCOUS SINTERING

As indicated in the previous section, the description of lunar breccia formation by viscous sintering in a stress-free environment requires a satisfactory description of sintering under various cooling conditions of interest. This question has been addressed during the grant by modifying the standard Frenkel treatment of viscous sintering appropriate for isothermal conditions. This model assumes radial hyperbolic flow during particle coalescence, and equates the rate of change of the surface energy with the rate of energy dissipation in viscous flow to obtain an expression for the rate of thicknening of the necks joining the particles.

In a modification of this analysis we have obtained an expression for the radius X of the neck at time t of particles of radius R which came in contact at time t_c:

$$X^2 = \frac{3\gamma R}{2\pi} \int_{t_c}^{t} \frac{dt'}{\eta[T(t')]} \tag{37}$$

where η is the viscosity and γ is the surface tension.

The corresponding time for significant sintering, t_s is given by:

$$\int_{t_c}^{t_s} \frac{dt'}{\eta[T(t')]} \approx \frac{R}{\gamma} \tag{38}$$

For the case of cooling at a constant rate for a material whose viscosity over the temperature range of interest can be approximated by an Arrhenius relation--i.e.

$$T(t) = T_o - at \tag{39}$$

and

$$\eta(T) = \eta_o \exp\ (A/T) \tag{40}$$

one obtains

$$\phi\left(\frac{A}{T_c}\right) = \phi\left(\frac{A}{T_s}\right) + \frac{\eta_o Ra}{A\gamma} \tag{41}$$

where

$$\phi(\xi) = \frac{\exp(-\xi)}{\xi^2}\ \left(1 - \frac{2}{\xi}\right) \tag{42}$$

In evaluating T_c, the minimum contact temperature, for the cooling curves of interest, one takes T_s as the intersection of the respective cooling curves with the CT curve corresponding to the degree of crystallinity observed in the lunar sample, or as zero (the latter for cooling rates which do not intersect the CT curve). The minimum contact temperatures estimated in this way for Lunar Composition 70019 have been shown in Ref. 23. For the cooling rate at which the lunar sample was estimated to have cooled (about 0.12 K min^{-1}), a minimum contact temperature of about 1360 K is evaluated from Eqn. (41). Hence contact of the matrix particles at any temperature above or somewhat below the liquidus is sufficient to produce substantial sintering.

For some physical situations of interest in the formation of lunar breccias, the cooling history would be better represented as logarithmic cooling rather than by the linear cooling of Eqn. (39). Such logarithmic

cooling can be represented as:

$$T = T_o - C \ln t \qquad (43)$$

In this case, the determination of the minimum contact temperature must be based upon the more general relation of Eqn. (38)--evaluated using numerical techniques--rather than Eqn. (42).

The accuracy and limitations of Frenkel model are discussed in Ref. 21. It was recognized that the sintering rate calculated on the basis of this model provides an underestimate of the time required to produce a completely-dense body; but it should provide a useful estimate of the time required to produce a significant degree of sintering--which is the critical quantity of interest in the description of breccia formation.

XIX. THERMAL HISTORIES OF BRECCIAS

The approach and results of the kinetic analysis of crystallization and viscous sintering can fruitfully be combined with detailed heat flow calculations for geometries of interest to elucidate in more detail the histories of lunar breccias. Specifically, calculations of the type presented previously by Jaeger and by Provost and Bottinga can provide useful estimates of the thermal histories for planar geometries. From such calculations it should be possible to set limits on the size of the bodies in which various breccias formed and on the nature of the cooling history which they experienced. Heat flow calculations were also carried out in our laboratory (see discussion below) on the model suggested by Simonds, in which the heat-sinking effects of fragmental material on the

initial cooling of the molten ejecta blanket are included. With such information, it was possible to distinguish with confidence between the disparate lithification mechanisms which were suggested for clastic breccias--viz., shock lithification and sintering in a stress-free environment. This approach was applied to a reasonable number of lunar breccias to obtain insights into thermal histories. These include lunar breccias 70019 and 79155 (described in Ref. 24); 15498 (described in Ref. 30); 67975 (described in Ref. 36) and 15286 (described in Ref. 37). In nearly all cases, it was concluded that the breccias formed by a process of viscous sintering; and the kinetic analysis was used to infer cooling rates at which the bodies formed as well as to set limits on the sizes of the cooling bodies. The conclusion concerning the formation of the breccias was supported by observations of the refractive indices of glasses found in the matrices of the breccias.

XX. SOLUTE PARTITIONING AND THERMAL HISTORY OF LUNAR ROCKS

As indicated above, the kinetic analysis of the breccia formation developed during the grant is directly applicable to breccias with partly glassy matrices. For other lunar rocks, it is preferable to estimate thermal histories from other kinetic analyses. During the grant, we developed methods for inferring thermal histories from the partitioning data is presented in Ref. 22. This method is based on the rule of thumb that the characteristic diffusion distance for various diffusive transport processes is $(Dt)^{1/2}$, where D is the diffusion coefficient and t is the time. For non-isothermal situations, the characteristic distance

$(Dt)^{1/2}$ is replaced by $[\int_o^t D(t')dt']^{1/2}$ where D is the smaller (controlling) diffusivity. From the equilibration data of Taylor, values of D could be obtained.

Consider now a lunar sample whose observed partitioning ratio (of Zr between the two phases) equals that of an isothermal laboratory partitioning experiment at temperature T_o. Let t_o be the time at which the sample was at the temperature T_o and t_f be some final time when the sample was cooled and all diffusive processes had ceased. In the electron microprobe analyses of the lunar samples, a characteristic distance x_c for diffusion from the grain boundaries is observed. This represents the region near the inter-phase contact within which the Zr content is effectively constant. It has then been argued that x_c is the characteristic diffusion distance for all diffusion which took place at temperatures below T_o:

$$x_c = \left[\int_{t_o}^{t_f} D(t')dt'\right]^{1/2} \qquad (44)$$

The rationale is that if cooling were faster, less partitioning could occur at the lower temperatures (over a region of size x_c) and the observed characteristic temperature would be higher, and vice versa. It is recognized that the accuracy of an analysis based upon this concept is limited; but it is sound as a rough method of estimating cooling rates.

In applying this approach to lunar rocks, a constant cooling rate a was assumed and the analysis was applied to the partitioning of Zr by the ilmenite and ulvöspinel. The analysis was applied to 6 rocks collected from Station 1 at Elbow crater: 15065, 15075, 15076, 15082, 15085 and 15086. The estimated cooling rates for these rocks are shown in the

table below.

Sample	Cooling rate (C day^{-1})
15065	3
15075	3
15076	6
15082	6
15085	7
15086	16

All of the Gabbros studied (15065, 15075, 15076 and 15085) have estimated cooling rates of less than 10C day^{-1}. These estimates are in good agreement with the calculations of Lofgren and his associates based on the duplication of textures in cooling rate experiments. While the two breccias (15082 and 15086) have apparent cooling rates of 6 and 16C day^{-1}, large σ errors were noted in the experimental data. This is a result of the admixing of several rocks types, and seems to indicate that any past-brecciation heating and cooling was not of sufficient magnitude to re-equilibrate completely the Zr partitioning of the oxides.

Recognizing the approximate nature of this analysis and the potential importance of partitioning data for elucidating the thermal histories of lunar rocks, an exact theoretical analysis was undertaken of solute partitioning under both isothermal and continuous cooling conditions. The results of the analysis for a finite layered solid under isothermal conditions are presented in Ref. 28. Formal analytical expressions were provided for the form of the concentration profile in each phase, as well as for the average composition of each phase. From even limited experimental data, it is possible to obtain considerable insight into the process of solute partitioning, as well as quantitative

estimates of the kinetic and thermodynamic factors which are important in partitioning.

While the isothermal results presented in Ref. 28 were useful and (being analytic) are enlightening as to functional dependences, an accurate determination of the cooling histories of terrestrial or lunar samples from data on solute partitioning requires a satisfactory theoretical description of partitioning under nonisothermal (continuous cooling) conditions. Such partitioning was analyzed numerically for the finite layered solid (the same geometry considered in the paper on isothermal partitioning), with results presented in Ref. 49.

This analysis involves solving the coupled diffusion equations

$$D_1(t) \frac{\partial^2 C_1(x,t)}{\partial x^2} = \frac{C_1(x,t)}{\partial t} \tag{45a}$$

$$D_2(t) \frac{C_2(x,t)}{\partial x^2} = \frac{C_2(x,t)}{\partial t} \tag{45b}$$

subject to a specified cooling history (which can be of any form).

In the initial work, it was assumed that the distribution of solute is uniform at high temperatures, and that as the temperature is lowered, the concentrations adjust so as to approach the equilibrium ratio at the interface. The only assumption made with respect to this ratio is that at the interface between the phases.

$$C_1(0,t) = K(T(t))\ C_2(0,t) \tag{46}$$

Since the flux must be the same on both sides of the interface; hence

$$D_1 \frac{\partial C_1(0,t)}{\partial x} = D_2 \frac{\partial C_2(0,t)}{\partial x} \tag{47}$$

Further, the concentration gradient must be zero at the centers of the grains; hence

$$\frac{\partial C_1(-R_1,t)}{\partial x} = 0 \qquad (48a)$$

$$\frac{\partial C_2(R_2,t)}{\partial x} = 0 \qquad (48b)$$

where $2R_1$ and $2R_2$ are the thicknesses of the grains.

In solving this problem with a computer, Eqns. (45), (47) and (48) were replaced by the backward difference analogs. As an example, Eqn. (45) takes the form:

$$D(t)\, C_{i-1,\, n+1} - C_{i,\, n+1} \left(2D(t) + \frac{(\Delta x)^2}{\Delta t}\right) +$$

$$D(t) C_{i+1,\, n+1} = -C_{i,\, n} \frac{(\Delta x)^2}{\Delta t} \qquad (49)$$

where n+1 is an unknown level in time and i is a point in space.

For the case of spherical grains, the problem was solved using spherical coordinates with similar boundary conditions and similar replacement of differential equations by their backward difference analogs. In both geometries, the problem was solved for a range of cooling rates from 0.3 to 300°C day^{-1}, with material constants appropriate for the partitioning of Zr between ilmenite and ulvöspinel. The program as written, however, is quite general and can be used to describe partitioning during continuous cooling in a variety of systems. Specific provision was made for a variety of forms of the cooling history and equilibrium partitioning ratio as a function of temperature, as well as

arbitrary values of the initial concentrations, diffusion coefficients and sizes of the phases. Provision was also made to invert the problem and obtain cooling rates from measured concentration profiles, or from average concentrations in the two phases, or from concentrations measured at specified points in the two phases.

XXI. HEAT FLOW IN IMPACT MELTS

As indicated above the kinetic treatment of breccia formation by viscous sintering can be used to elucidate in detail the histories of lunar breccias. This is most fruitfully done by combining the results of the kinetic analysis with detailed heat flow calculations for geometries of interest. Of particular note in this regard is the model suggested by Simonds and his associates in which the heat-sinking effects of fragmental material on the initial cooling of a molten ejecta blanket are included.

This model was developed to explain the phase morphologies in the boulder from Apollo 17 Station 6, and suggested that the boulder represents a single impact melt sheet with differences in matrix texture and observed clast content correlating with different positions in the melt sheet. The melt sheet was suggested to consist of a mixture of superheated silicate liquid produced at the impact site and relatively cold clasts, not exposed to high shock pressures. Once mixed, the clasts and melt interact both thermally and chemically. The fine grain size, large quantity, and even distribution of clasts allows them to absorb heat rapidly, both as sensible heat and as the heat of fusion. Once the clasts and molten liquid come to local thermal equilibrium, further loss of heat takes

place by conduction and radiation to the surroundings. The latter rate of heat loss is expected to be smaller by orders of magnitude than that which results from the initial rapid cooling involving the clasts as heat sinks.

Analysis of the heat flow problem for a melt-clast mixture of the type suggested by Dr. Simonds was carried out under the grant. In this work, which was carried out in collaboration with Dr. Simonds, a number of modifications were added to the heat flow problem for a cooling slab described and solved analytically by Jaeger and solved numerically (in somewhat modified form) by Provost and Bottinga--in addition to providing a description of heat flow to clasts distributed through a melt.

The physical situation during cooling was divided into two separate heat flow problems, one appropriate at short times when the melt cools very rapidly because of the presence of the clasts, and the second appropriate at long times when the blanket cools more slowly through the region of crystallization. Both problems were solved numerically for physical situations of interest.

Clasts having a given (cold) initial temperature are randomly located in a hot melt. The clasts have a log normal size distribution, with a median size of 0.1 mm and a standard deviation of log 4 (values typical of an immature lunar soil). The clasts are all assumed to melt at a single liquidus temperature of 1310 C (that determined for the 14310 composition).

The calculations indicate: (1) thermal equilibration of a hot melt-cold clast system takes place quite rapidly, with equilibration times in the range of 100 sec. being typical for clasts having the indicated size

distribution; (2) the average temperature of the melt-clast system during the initial portion of first-stage cooling decreases approximately logarithmically with time; (3) the time of equilibration of the melt-clast system increases as the square of the mean clast size; (4) many clasts are partially melted at the end of first-stage cooling; (5) the distribution of clast types as well as their sizes can have a profound effect on the extent of clast digestion--with changes as large as an order of magnitude being observed in the volume fraction of clasts remaining after first-stage cooling; (6) small, isolated clasts even of the most refractory type tend to be digested; and (7) there is more clast digestion than if all such digestion took place at the final equilibration temperature.

The preferential melting of small clasts and its effect on the average clast size are illustrated by the following results: For a melt with an initial temperature of 1400°C, a mixture containing 41% clasts with a mean initial size of 154 μm becomes after equilibration a mixture of 30% clasts with a mean size of 200 μm. For a higher initial melt temperature of 1600°C, the same clast distribution yields, after equilibration, a mixture of 18.5% clasts with a mean size of 180 μm. At the higher initial temperature, there is more digestion of large clasts than at the lower temperature, and hence the increase in mean clast size is smaller.

The second-stage cooling, which involves heat flow from the melt to its surroundings, takes place on a time scale which is typically larger by orders of magnitude than the time of thermal equilibration in first-stage cooling. In describing such cooling the rock beneath the melt sheet has been taken as cold material with the same thermal properties as the melt sheet. For the boundary condition above the melt sheet,

three possibilities have been considered: (1) the melt sheet is covered with a thick cold blanket (conduction); (2) the melt sheet represents a surface flow with no insulating layer above it (radiation); and (3) the melt sheet is covered by a thin, cold insulating layer, such as would be expected if debris from the impact event immediately fell on top of the melt sheet (conduction + radiation).

The calculations for second-stage cooling were used to provide information about the cooling rates at different temperatures and various locations in the melt sheet, as well as the times required for various parts of the sheet to cool to selected temperatures of interest.

The results of these calculations indicate that: (1) cooling by heat flow to the surroundings takes place on a time scale which typically is larger by orders of magnitude than the time of thermal equilibration in first-stage cooling; (2) for a melt sheet with thick insulation both above and below, the time to cool to a given temperature increases as the square of the distance from the boundaries of the melt sheet--but only for a sufficiently limited range of temperature and distance from the boundary that the finite extent of the melt sheet is not significant; and (3) when greater ranges of temperature and time are considered, the time to cool to a given temperature increases less rapidly with distance from the boundary than predicted for an infinite body.

The results of the calculations as applied to the Apollo 17 Station 6 Boulder are presented in Ref. 32, and applied to the Manicouagan melt sheet in Ref. 44. In the case of the Manicouagan melt sheet, the flow was modelled as a 200 meter thick slab covered by a thick blanket

of cold debris. The results of the calculations indicate that crystallization should have been complete throughout the sheet in about 1600 years; while the outer 3.5 m. should have crystallized in about 6.6 years. The results for a melt with an initial temperature difference of 200°C across the sheet, and also for a melt sheet covered by a warm (400°C) blanket on top are not significantly different from those for a melt with a uniform initial temperature, covered by a cold (0°C) blanket on top.

Results of the heat flow calculations for both the first and second stages of cooling have also been applied to the formation of lunar breccias. In particular, it has been suggested that if the cooling rate during first-stage cooling is sufficiently high that the nose in the continuous cooling curve for the matrix material is avoided, and if the equilibration temperature is sufficiently low that detectable crystallization does not take place during the much slower second-stage cooling, then a glassy matrix breccia can be formed. With progressively slower cooling and higher equilibration temperatures, breccias with partly crystalline matrices and eventually completely crystallized rocks will be formed. Further, if the equilibration temperature at the end of first-stage cooling is appreciably above the nose of the continuous cooling curve (see third Section below), the much slower cooling expected for sedond-stage cooling, save in the regions near the boundaries of the melt sheet, sets severe limitations on the size of the bodies which can be formed with a given degree of partial crystallinity. Examples of such applications of the heat flow analysis are given in Refs. 36 and 37 for the 15286 and 67975 breccias and in Ref. 30 for the 15498 breccia.

XXII. THERMAL HISTORIES OF OLIVINES

As a natural extension of our work of solute partitioning between phases in a solid body, an analysis was undertaken of diffusive homogenization in olivines. This was motivated by the fact that olivines in both lunar and terrestrial rocks are often compositionally zoned, and the composition profiles can be used to estimate the rates at which the rocks cooled. In the initial analysis, the minimum cooling rate consistent with the preservation of observed zoning in an olivine grain was determined. Our work in this area was carried out in collaboration with Professor Taylor of the University of Tennessee.

It was recognized that the extent to which a grain approaches equilibrium during cooling depends upon the "as-solidified" concentration profile, as well as upon the cooling rate. Lacking information about the as-solidified concentration profile, it was assumed that at the solidus there was a step-function in the forsterite concentration within the grain, from an Fo-rich core to a Fa-rich rim. This assumption directed attention to the minimum cooling rate associated with the preservation of a given gradient since a system with an initial gradient would equilibrate more rapidly than one with a step-function profile.

It was also assumed that there is no flux across the center of the grain, and that the grain is effectively a closed system (there is no flux across the grain boundary). Attention was specifically directed to a finite system, and provision was made for a concentration-dependent diffusivity (in accord with measurements on the system). The appropriate diffusion equation was solved for both plate and spherical geometries.

These are:

$$\text{(a)}\quad \underline{\text{PLATE}}\quad \frac{\partial C}{\partial t} = \frac{\partial}{\partial X}\left\{\tilde{D}[C(X),\ P_{O_2}(T),\ T(t)]\ \frac{\partial C}{\partial X}\right\} \tag{50a}$$

$$\text{(b)}\quad \underline{\text{SPHERE}}\quad \frac{\partial C}{\partial t} = \frac{1}{r^2}\frac{\partial}{\partial r}\left\{r^2\ D[C(r),\ P_{O_2}(T),\ T(t)]\ \frac{\partial C}{\partial r}\right\} \tag{50b}$$

where C is the mole fraction of fayalite and D is the interdiffusion coefficient.

The data of Buening and Buseck on Fe-Mg interdiffusion in the olivines indicate that $\tilde{D}$ depends on crystallographic direction, as well as on temperature, composition and P_{O_2}. Consistent with our concern for minimum cooling rates, $\tilde{D}$ was taken as that in the a direction, which is slower by about a factor of 4 than that in the c direction. The interdiffusion coefficient was then taken as:

$$\tilde{D} = 25P_{O_2}^{1/6} \exp\left(-0.0501\ X_{Fe_2SiO_4} - 14.03\right) \exp\left[-\frac{1.373\text{eV} - 0.0095X_{Fe_2SiO_4}}{kT}\right] \tag{51}$$

with the oxygen partial pressure taken as that suggested by Sato et al. for lunar conditions, about 0.5 log atm. below the iron-wustite buffer:

$$\log_{10}P_{O_2} = 0.015T(K) - 34.6 \tag{52}$$

The diffusion equation [Eqn. (50a) or (50b)] was solved by replacing it with its finite difference analog, applying the boundary conditions, and solving the resultant set of simultaneous equations by the Thomas tridiagonal method. Due to the non-linearity of the equation, it was necessary to iterate the procedure to approach the correct solution.

Diffusion profiles were calculated for several sets of initial conditions and cooling rates, and were compared with profiles measured

by Professor Taylor in olivine grains from Lunar Samples 12002 and 15555. The results are given in Ref. 38. Again in accord with our concern for minimum cooling rates, the largest compositionnl gradients found in the olivine crystals of a particular sample were used for this analysis.

For cooling rates of interest (consistent with the measured profiles), the results of calculations for the plate geometry did not differ significantly from those for the spherical geometry. By comparing the measured profiles with those calculated for various cooling rates, a minimum cooling rate of about 10°C day^{-1} was suggested for 12002, and a minimum cooling rate of about 5°C day^{-1} for 15555. These minimum values compare well with cooling rates of 10-20°C day^{-1} estimated by other workers from controlled crystallization studies on both these rocks.

Considering the step-function initial concentration profiles assumed in the analysis, which directed our concern to minimum cooling rates, the agreement in form between the calculated and measured profiles was pleasantly surprising.

Also at the Eighth Lunar Science Conference, Walker et al. presented a different approach to calculating cooling rates from compositional profiles in olivines. They neglected the compositional dependence of the diffusion coefficient and assumed an initial compositional profile in the grain where the concentration varies as exp $(-Br^3)$. As in our original analysis, homogenization of the initial profile was assumed to begin at some closure temperature. A detailed comparison of the predictions of the two models is presented in Ref. 46. It was found that both approaches underestimate the cooling rate corresponding to a given gradient in composition; and it was suggested that both can be used to provide order-of-magnitude estimates

of the cooling rates. Other treatments of diffusional homogenization are required if more detailed information about the thermal history is desired.

A first approach to providing such detailed information is presented in Ref. 43. The model represents a first-effort attempt to calculate the "as-solidified" compositional profile in an olivine grain. Being a numerical treatment, it takes proper account of the dependence of the diffusion coefficient in the solid on composition and oxygen partial pressure, and is capable of treating the effects of crystallographic orientation. Most importantly, it includes consideration of diffusional homogenization which takes place during solidification as well as that which takes place after solidification is complete. Using approximate growth rate data on a high-FeO olivine with this analysis, the results shown in Ref. 43 were obtained for a LUNA 24 olivine. As shown there, the calculated profile for a cooling rate of 2°C day^{-1} agrees well with the measured profile.

The principal limitations to this model lie in its assumption that the growth rate is independent of time at a given temperature, that the melt is well-stirred, and that the size of the melt is that which gives an olivine grain of the observed size when the liquid is depeleted in MgO. Considering the large volume change involved in solidification, and the concomitant possibility of diffusion-controlled growth, the growth rate could well be time-dependent. The assumption of a well-stirred melt, with the accompanying neglect of compositional gradients in the liquid, may be appropriate for the growth of some olivine crystals. In other cases, however, the neglect of compositional gradients in the liquid at the crystal-liquid interface, as would be expected for diffusion-controlled

growth, will be important. The related assumption of specifying the size of the volume from which the grain grows is also closely linked to the assumption of stirring in the melt.

It is difficult to assess with any confidence the effects of each of these assumptions on the predicted cooling rates. It seems, however, that the combined effects of the uncertainties in the analysis would render its accuracy similar to that of the initial treatments which considered homogenization on cooling below some closure temperature. That is, the analysis should be taken as yielding predictions of cooling rates with order-of-magnitude accuracy. The approach does, however, direct attention to the nature of "as-solidified" compositional profiles, and these are discussed at greater length in Ref. 46.

In that paper, the initial formulation of a model is presented which describes diffusional homogenization of an olivine grain growing from a liquid which is cooling at a constant rate. In this model, the possibility of compositional gradients existing in both liquid and solid during solidification is considered. This represents a more realistic attempt to describe the origin of the compositional gradients observed in olivine crystals. In the model, it is assumed that the growth of the crystals is controlled initially by interface kinetics. This would be the case for small crystal sizes or fast crystallization kinetics. After some period of growth, it is expected that the liquid near the interface will become depleted in the constituents of the crystal such that the flux of MgO or FeO to the interface will no longer be sufficient to maintain the constant growth rate. A boundary layer is then developed in the liquid adjacent to the interface, the growth rate decreases, and the growth becomes limited by diffusion in the liquid.

In detail, the olivine grain is assumed to grow from a sphere of liquid whose radius is half the average distance between olivine grains. Growth continues until the liquid is depleted by an amount equal to the amount of MgO in the olivines observed in a given rock. Taking Lunar rock 15555 as an example, about 10% of the rock is olivine having an average MgO content of about 40 mole %. The average liquid concentration of MgO in the surrounding liquid sphere would, therefore, be decreased by about 4 mole % during crystallization of this olivine. It is also assumed that after growth is complete, there is no further communication between the olivine grain and its surroundings. Diffusion continues within the grain until it is homogenized or until it cools to a temperature below which no significant diffusion takes place at the imposed cooling rate.

Experimental data on average growth rates of a high-iron analogue of Lunar rock 15555 were obtained. The growth rate data indicate that the growth process must indeed be dependent on time. From the average growth rates and the model for diffusion-controlled growth, together with composition profiles determined in the liquid, the diffusion coefficients of FeO and MgO in the melt were estimated as functions of temperature.

This model of diffusional homogenization of olivine takes account of diffusion in both liquid and solid during solidification, as well as diffusion in the solid after solidification is complete. The analysis has been applied to date to crystals nucleated at 1272°C and indicates the development of only small compositional gradients in the crystals. These results are in accord with the experimental data on olivine crystals grown in the laboratory from this composition at high temperatures. It has not yet been established which modifications of the assumptions in

the model will be required to describe the composition gradients which are observed in a variety of olivine crystals; but the temperature at which crystallization is initiated and the nature of the phases crystallizing at a given time seem to be important factors for future analysis. These and other modifications of the model--including the effects of a diffusional boundary layer at the interface with convection in the bulk liquid--are presently being explored.

PUBLICATIONS

NASA GRANT NGR 22-009-646

1. D.R. Uhlmann, "A Kinetic Treatment of Glass Formation", J. Non-Cryst. Solids 7, 337-348 (1972).

2. M. Cukierman, P.M. Tutts and D.R. Uhlmann, "Viscous Flow Behavior of Lunar Compositions 14259 and 14310", in Proceedings of the Third Lunar Science Conference (Supplement 3, Geochim. et Cosmochim, Acta) Vol. 3, pp. 2619-2625 (MIT Press, 1972).

3. G. Scherer, R.W. Hopper and D.R. Uhlmann, "Crystallization Behavior and Glass Formation of Selected Lunar Compositions", in Proceddings of the Third Lunar Science Conference (Supplement 3, Geochim, et Cosmochim, Acta) Vol. 3, pp. 2627-2637 (MIT Press, 1972).

4. M. Cukierman and D.R. Uhlmann, "Viscous Flow of Lunar Compositions", in The Apollo 15 Lunar Samples, pp. 57-59 (Lunar Science Institute, 1972).

5. G. Scherer and D.R. Uhlmann, "Crystallization Behavior of -phenyl o-cresol", J. Crystal Growth 15, 1-10 (1972).

6. D.R. Uhlmann, M. Cukierman, G. Scherer and R.W. Hopper, "Viscous Flow, Crystallization Behavior and Thermal History of Orange Soil Material", Trans. A.G.U. 54, 617-618 (1973).

7. M. Cukierman and D.R. Uhlmann, "Viscosity of Liquid Anorthite", J. Geophys. Res. 78, 4920-4923 (1973).

8. R.W. Hopper and D.R. Uhlmann, "Temperature Distributions during Crystallization at Constant Velocity", J. Crystal Growth 19, 177-186 (1973).

9. M. Cukierman, L. Klein, G. Scherer, R.W. Hopper and D.R. Uhlmann, "Viscous Flow and Crystallization Behavior of Selected Lunar Compositions", in Proceedings of the Fourth Lunar Science Conference (Supplement 4, Geochim. et Cosmochim. Acta) Vol.3, pp. 2685-2696 (Pergamon Press, 1973).

10. M. Cukierman, J.W. Lane and D.R. Uhlmann, "High Temperature Flow Behavior of Glass-Forming Liquids: a Free Volume Interpretation", J. Chem. Phys. 59, 3639-3644 (1973).

11. R.W. Hopper and D.R. Uhlmann, "Solute Redistribution During Crystallization at Constant Velocity and Constant Temperature", J. Crystal Growth 21, 203-213 (1974).

12. M. Cukierman and D.R. Uhlmann, "Effects of Iron Oxidation State on Viscosity, Lunar Composition 15555", J. Geophys. Res. 79, 1594-1598 (1974).

13. R.W. Hopper, G. Scherer and D.R. Uhlmann, "Crystallization Statistics, Thermal History and Glass Formation", J. Non-Cryst. Solids 15, 45-62 (1974).

14. R.W. Hopper and D.R. Uhlmann, "On Diffusive Creep and Viscous Flow", Materials Science and Engineering 15, 137-144 (1974).

15. D.R. Uhlmann, L. Klein, G. Kritchevsky and R.W. Hopper, "The Formation of Lunar Glasses", in Proceedings of the Fifth Lunar Science Conference (Supplement 5, Geochim. et Cosmochim. Acta) Vol. 3, pp. 2317-2331 (Pergamon Press, 1974).

16. R.W. Hopper, P. Onorato and D.R. Uhlmann, "Thermal Histories and Crystal Distributions in Partly Devitrified Lunar Glasses Cooled by Radiation", in Proceedings of the Fifth Lunar Science Conference (Supplement 5, Geochim. et Cosmochim. Acta) Vol. 3, pp. 2257-2274 (Pergamon Press, 1974).

17. G. Scherer, D.R. Uhlmann, C.E. Miller and K.A. Jackson "Crystallization Behavior of High Purity o-terphenyl", J. Crystal Growth 23, 323-330 (1974).

18. L. Klein and D.R. Uhlmann, "Crystallization Behavior of Anorthite", J. Geophys. Res. 79, 4869-4874 (1974).

19. G.W. Scherer and D.R. Uhlmann, "Crystallization Kinetics of $Na_2O \cdot 3SiO_2$", J. Crystal Growth 29, 12-18 (1975).

20. D.R. Uhlmann, "Crystal Growth and Glass Formation", in Mass Transport Phenomena in Ceramics, pp. 465-478 (Plenum, 1975).

21. D.R. Uhlmann, L. Klein and R.W. Hopper, "Sintering, Crystallization and Breccia Formation", The Moon 14, 277-284 (1975).

22. L. A. Taylor, D.R. Uhlmann, R.W. Hopper and K.C. Misra, "Absolute Cooling Rates of Lunar Rocks: Theory and Application", in Proceedings of the Sixth Lunar Science Conference, Vol. 1, pp. 181-191 (Pergamon Press, 1975).

23. D.R. Uhlmann, L. Klein, P.I.K. Onorato and R.W. Hopper, "The Formation of Lunar Breccias: Sintering and Crystallization Kinetics", in Proceedings of the Sixth Lunar Science Conference, Vol. 1, pp. 693-705 (Pergamon Press, 1975).

24. L. Klein, P.I.K. Onorato, D.R. Uhlmann and R.W. Hopper, "Viscous Flow, Crystallization Behavior and Thermal Histories of Lunar Breccias 70019 and 79155", in Proceedings of the Sixth Lunar Science Conference, Vol. 1, pp. 579-593 (Pergamon Press, 1975).

25. G.W. Scherer and D.R. Uhlmann, "Diffusion-Controlled Growth of Dendrite Arrays", J. Crystal Growth 30, 304-310 (1975).

26. G.W. Scherer and D.R. Uhlmann, "Effects of Phase Separation on Crystallization Behavior", J. Non-Cryst. Solids 21, 199-213 (1976).

27. G.W. Scherer and D.R. Uhlmann, "Diffusion Controlled Crystal Growth in K_2O-SiO_2 Compositions", J. Non-Cryst. Solids 23, 59-80 (1977).

28. R.W. Hopper and D.R. Uhlmann, "Diffusive Isothermal Partitioning in a Layered Medium, with Geologic Applications", J. Geophys. Res. 81, 5721-5730 (1976).

29. P.I.K. Onorato and D.R. Uhlmann, "Nucleating Heterogeneities and Glass Formation", J. Non-Cryst. Solids 22, 367-378 (1976).

30. D.R. Uhlmann and L.C. Klein, "Crystallization Kinetics, Viscous Flow and Thermal Histories of Lunar Breccias 15286 and 15498", in Proceedings of the Seventh Lunar Science Conference, Vol. 2, pp. 2529-2541 (Pergamon Press, New York, 1976).

31. L.C. Klein and D.R. Uhlmann, "The Kinetics of Lunar Glass Formation, Revisited", in Proceedings of the Seventh Lunar Science Conference, Vol. 1, pp. 1113-1121 (Pergamon Press, New York, 1976).

32. P.I.K. Onorato, D.R. Uhlmann and C.H. Simonds, "Heat Flow in Impact Melts: Apollo 17 Station 6 Boulder and some Applications to other Breccias and Xenolith-laden Melts, in Proceedings of the Seventh Lunar Science Conference, Vol. 3, pp. 2249-2267 (Pergamon Press, New York, 1976).

33. D.R. Uhlmann and A.G. Kolbeck, "Phase Separation and the Revolution in Concepts of Glass Structure", Phys. Chem. Glasses 17, 146-158 (1976).

34. D.R. Uhlmann, "The Stability of Glasses, with Special Reference to Disposal of Radioactive Wastes", in Disposal of Radioactive Wastes pp. 121-138 (ERDA, Washington, 1977).

35. D.R. Uhlmann, "Glass Formation", in Proceedings of XI International Congress on Glass, Vol. 1, pp. 43-85 (International Congress on Glass, Prague, 1977).

36. D.R. Uhlmann, L.C. Klein and C.A. Handwerker, "Crystallization Kinetics, Viscous Flow and Thermal History of Lunar Breccia 67975", in Proceedings of the Eighth Lunar Science Conference, Vol. 2, pp. 2067-2078 (Pergamon Press, New York, 1977).

37. C.A. Handwerker, L.C. Klein, P.I.K. Onorato and D.R. Uhlmann, "Matrix Glass vs. Intruded Glass in Lunar Breccia 15286", in Proceedings of the Eighth Lunar Science Conference, Vol. 2, pp. 2581-2592 (Pergamon Press, New York, 1977).

38. L.A. Taylor, P.I.K. Onorato and D.R. Uhlmann, "Cooling Rate Estimations Based on Kinetic Modeling of Fe-Mg Diffusion in Olivine", to appear in Proceedings of the Eighth Lunar Science Conference, Vol. 2, pp. 1581-1592 (Pergamon Press, New York, 1977).

39. L.C. Klein, C.A. Handwerker and D.R. Uhlmann, "Nucleation Kinetics of Sodium Disilicate", J. Crystal Growth, 42 (1977) 47-51.

40. D.R. Uhlmann and R.W. Hopper, "Relaxation in Glasses", in Metallic Glasses, pp. 128-160 (American Society for Metals, Cleveland, 1977)

41. D.R. Uhlmann, "Glass Formation", J. Non-Cryst. Solids 25, 42-85 (1977). Same paper as Ref. 34, published with other review lectures from ICG IX in special volume of the Journal.

42. C.A. Handwerker, P.I.K. Onorato and D-R. Uhlmann, "Viscous Flow, Crystal Growth & Glass Formation of Hsghland and Mare Basalts from LUNA 24", in Mare Crisium: The View from Luna 24, pp. 483-493 (Pergamon Press, 1978).

43. L.A. Taylor, P.I.K. Onorato, D.R. Uhlmann and R.A. Coish, "Subophitic Basalts from Mare Crisium: Cooling Rates", in Mare Crisium: The View from Luna 24, pp. 473-481 (Pergamon Press, 1978).

44. P.I.K. Onorato, D.R. Uhlmann and C.H. Simonds, "The Thermal History of the Manicouagan Impact Melt Sheet, Quebec", J. Geophys. Res. 83, 2789-2798 (1978).

45. D.R. Uhlmann, C.A. Handwerker, D. Goncz and P.I.K. Onorato, "The Formation Kinetics of Lunar Glasses", in Proceedings of the Ninth Lunar and Planetary Science Conference, Vol. 2, pp. 1527-1536 (Pergamon Press, 1978).

46. P.I.K. Onorato, D.R. Uhlmann, L.A. Taylor, R.A. Coish and R.P. Gamble, "Olivine Cooling Speedometers", in Proceedings of the Ninth Lunar and Planetary Science Conference, Vol. 1, pp. 613-628 (Pergamon Press, 1978).

47. R.J. Kirkpatrick, L. Klein, D.R. Uhlmann and J.F. Hays, "Rates and Processes of Crystal Growth in the System Anorthite-Albite, J. Geophys. Res. 84, 3671-3676 (1979).

48. D.R. Uhlmann, "Glass Formation, a Kinetic Phenomenon", to appear in Proceedings of IX All-Union (USSR) Conference on the Glassy State.

49. M.C. Weinberg, P.I.K. Onorato and D.R. Uhlmann, "The Behavior of Bubbles in Glass Melts: I. Dissolution of a Stationary Bubble Containing a Single Gas", accepted for publication, J. Am. Ceram. Soc.

50. P.I.K. Onorato, H. Yinnon, D.R. Uhlmann and L.A. Taylor, "Partitioning as a Cooling Rate Indicator", to appear in Proceedings of the Tenth Lunar and Planetary Science Conference.

51. D.R. Uhlmann, P.I.K. Onorato and G.W. Scherer, "A Simplified Model for Glass Formation", to appear in Proceedings of the Tenth Lunar and Planetary Science Conference.